Proceeding of the 13th International Conference on QIR (Quality in Research)
Yogyakarta, Indonesia, 25-28 June 2013
ISSN 1411-1284

A Modified Rotor Model to Approach the Dynamic Responses of Anisotropic Rotor with Different Shaft Orientation

Jhon Malta

Department of Mechanical Engineering, Faculty of Engineering,
AndalasUniversity, KampusLimauManis Padang25163
E-mail :jhonmalta@ft.unand.ac.id

ABSTRACT

This research deals with a modification of anisotropic rotor model in order to approach the experimental results of the dynamic responses of anisotropic rotor. The prototype of an anisotropic rotor with two disks is supported by four quasi-rigid bearings. In the experimental studies, the dynamic responses of disks are recorded in horizontal and vertical directionsat constant angular speed from 1 to 80 Hz with an incremental speed of 1Hz. In the numerical studies, two mathematical models are developed by using a minimal number of discrete elements. The dynamic responses of the models are solved by using the Runge-Kuttamethod of fourth order. In the first model, the mass of shaft is negligible. In the second model, the mass of shaft is taken into account. Comparing the numerical and the experimental results, the natural frequencies of the numerical results of the first model is rather higher than the experimental results. The better results which closed to the experimental results are obtained in the second rotor model, whereas the mass of shaft contributes to reduce the natural frequencies. In the other results, the dynamic responses of the rotor both in simulation and in experiment show the instability area in a wide range.

Keywords
Anisotropic rotor, shaft orientation, Runge-Kutta method

1. INTRODUCTION

Many rotor models have been developed in order to investigate the real rotors in industry fields [1]-[7]. For a simple real rotor, a Jeffcott rotor model can be used to approach the rotor, but for a more complicated rotor system, it must be modeled by a more complicated rotor model too. In case of an anisotropic rotor, the directions of principal axes of shaft cross sections can be different along the shaft. Especially in case of a twisted anisotropic rotor, the directions of principal axes of cross sections change along the shaft. In this case, the rotor model must be modeled by discrete elements [8]. Actually, some existing methods e.g. finite element methodcan be used to develop the mathematical rotor model [9]-[11]. However, those methods should be modified due to the existing of the different element orientations along the shaft. In this paper, an alternative method is developed by using strain energy method for asymmetric bending of a beam in order to obtain the minimum number of shaft elements of rotor model.

An anisotropic rotor can be modeled in fixed or rotating reference frame. In fixed reference frame, the shaft stiffness of rotor model varies with time. In the rotating reference frame, the differential equations are speed-dependent. In dynamic analysis, the time-variant system is more complicated than the speed-dependent system. However, in the speed-dependent rotor system, the dynamic analysis should be simulated step by step at each frequency. The dynamic responses of the rotor model are solved by using the Runge-Kutta method. Further, the amplitudes of the dynamic responses of the rotor model are benchmarked by the experimental results.

2. DESCRIPTION OF THE ROTOR

2.1 Prototype of the rotor

In this research, the dynamic behavior of the rotor is investigated both in experimental and numerical simulation analyses. In the experimental studies, a prototype of the anisotropic rotor has been designed and manufactured as depicted in figure 1. The main rotor consists of a steel shaft (X90CrMoV18) with a diameter 8 mm and a total length of 626 mm. Nevertheless, the effective shaft length is assumed 540 mm that is the shaft length between the first bearing and the fourth bearing. The shaft is divided into three sections, in which each section has a 180 mm of shaft length. Along 166 mm of the shaft section the thickness of the cross section is 5 mm. The three sections of anisotropic shaft have different orientationsof shaft with the orientation of each section is defined to be $\beta_1=0^o$, $\beta_2=30^o$, and $\beta_3=60^o$, respectively. Two rigid disks are attached on the shaft. Each disk has 1.153 kg of mass. The ratios of mass moment of inertia are $\Theta_{p1}= \Theta_{p2}=1.90$. Near of each disk, an external damper is attached on the shaft. The main rotor is supported by four quasi-rigid bearings. The type of bearings isself-aligning ball bearing.The dynamic responses of the rotor are recorded by using two eddy current displacement sensors at each disk, in which the V-position of two sensors spans an angle of 90^o. The displacement of disk in horizontal and vertical direction can be measured by using a rotary transformation of 45^o.

ISSN 1411-1284

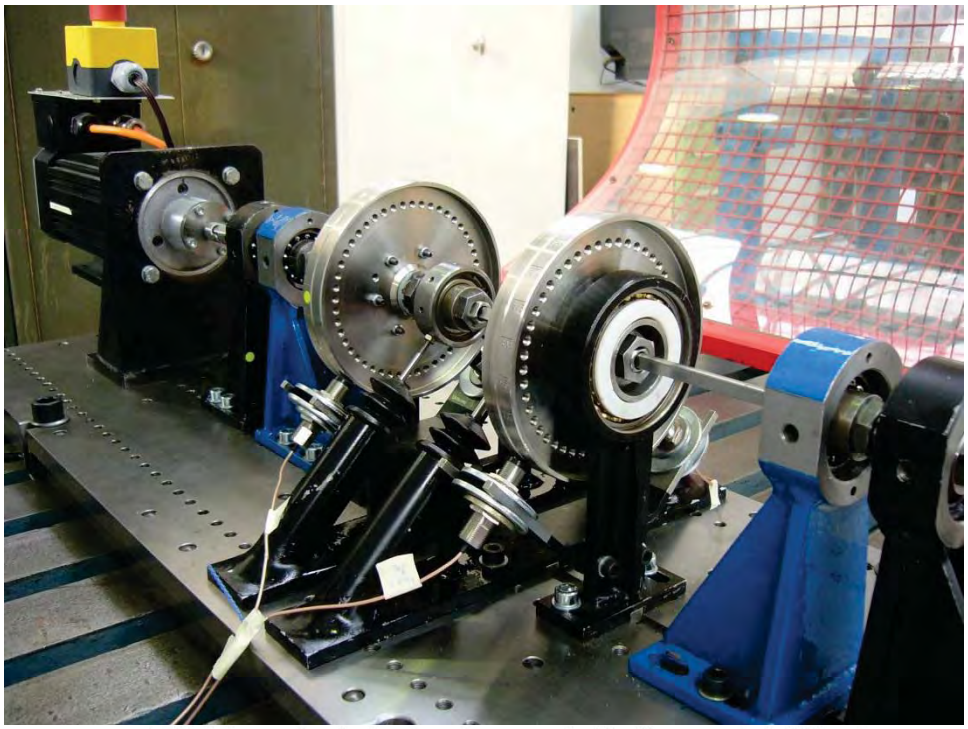

Figure 1: Prototype of anisotropic rotor supported by four quasi-rigid bearings

The rotor is operated at constant angular speed from 1 Hz until 80 Hz with an incremental speed of 1 Hz. The signals of the four displacement sensors are acquired by using the dSpace hardware type DS1103. The MATLAB software is used to control the dSpace and to process the signal data. The signals are filtered by a fourth order lo-pass butterworth filter in MATLAB with a cut off frequency at 100 Hz. The experimental data in time domain are transformed into the frequency domain by using Fast Fourier Transform (FFT).

2.1 Mathematical models of the rotor

Generally, the differential equations of rotor motion can be derived both in a fixed and rotating reference frame. If the rotor is modeled in a rotating reference frame, where the coordinate system follows the rotation of the shaft, then the differential equations of the system become speed-dependent. Hence, at constant rotational speed, the dynamic parameters of the rotor can be considered constant.

Furthermore, based on the experimental test-rig, whereas the two disks rotor system is supported by four quasi-rigid bearings must be modeled by multi degrees of freedom of rotor model. By using the minimal number of discrete shaft elements, for the first mathematical rotor model, the shaft is dividedinto five discrete elements as shown in figure 2. The parameters of the rotor model 1 are listed in table 1. The mass of shaft is negligible. The shaft orientationsof the shaft element 1 and 2 are $\beta_1=\beta_2=0^o$.Further, the shaft orientations of the shaft elements 3,4, and 5 are $\beta_3=30^o$, $\beta_4=\beta_5=60^o$, respectively. For external damper, an approach of proportional damping due to absolute velocity of disk can be used. In the rotor model1, the coefficients of the proportional external damping and internal damping are assumed d_a=0.18 and d_i=0.001, respectively. Furthermore, the differential equations of the rotor motion can be arranged as in [12]-[13] as

$$[[M_T]+[M_G]]\{\ddot{q}_W\}+[[D_T]+[D_G]+[D_a]+[D_i]]\{\dot{q}_W\}+[[K_T]+[K_G]+[K_a]+[K_W]]\{q_W\}=\{\{p_T\}+\{p_a\}+\{p_g\}\} \quad (1)$$

or in a simple form, the eq.1 is written as

$$[M]\{\ddot{q}_W\}+[D]\{\dot{q}_W\}+[K]\{q_W\}=\{p\}, \quad (2)$$

where[M], [D], and [K]are mass, damping, and stiffness matrices, respectively. These matrices are 4Nx4N of matrix size, with N is the number of disk. The $\{q_W\}$ isthe column matrix of displacement of disks and the $\{p\}$ is the force column matrix. The subscript T and G are to define the derivation matrices of translatory inertia and rotary inertia, respectively. Further, the [D_a], [D_i], and [K_a] are the external damping, internal damping, and proportional stiffness matrix of derivation of external damping matrix, respectively.

ISSN 1411-1284

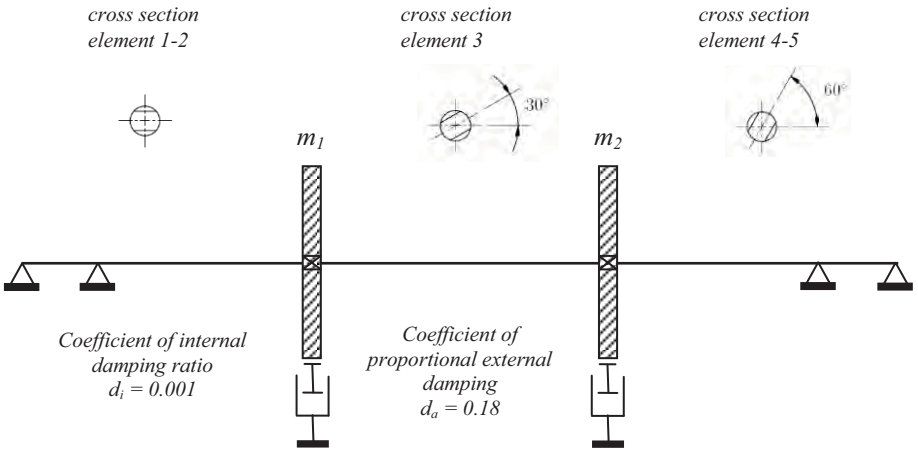

Figure 2: Mathematical model 1 of the rotor (mass of shaft is negligible)

Table 1: Parameter of discrete shaft element (model 1).

No. element	Length of element [m]	Modulus of elasticity [MPa]	Orientation of shaft element [degree]	Mass of disk/shaft element [kg]	Polar mass moment of inertia, Θ_p [kgm^2]	Axial mass moment of inertia, Θ_a [kgm^2]
1	0.050	210E+9	0	-	-	-
2	0.130	210E+9	0	-	-	-
-	-	-	-	m_1= 1.153	0.002572	0.001356
3	0.180	210E+9	30	-	-	-
-	-		-	m_2 = 1.153	0.002572	0.001356
4	0.130	210E+9	60	-	-	-
5	0.050	210E+9	60	-	-	-

Furthermore, the stiffness matrix $[K_W]$ can be arranged based on the Strain-Energy method [14]. The mathematical model in figure 2 is solved to obtain the reaction forces of all supports and the distribution of bending moment for each force or external bending moment acting at node.

For the second mathematical rotor model, the mass of shaft is taken into account. The mass of each discrete shaft element in the rotor model 1 is assumed as small and very thick disk as shown in figure 3 and the parameter of these shaft elements in table 2. Because a disk must be attached at a node, thus a point of mass of shaft element is placed in the center of each discrete shaft element; therefore, in the rotor model 2 a discrete shaft element as in the model 1 is divided into two discrete shaft elements. The other parameters in the rotor model 1 are the same with the parameters in the model 2.

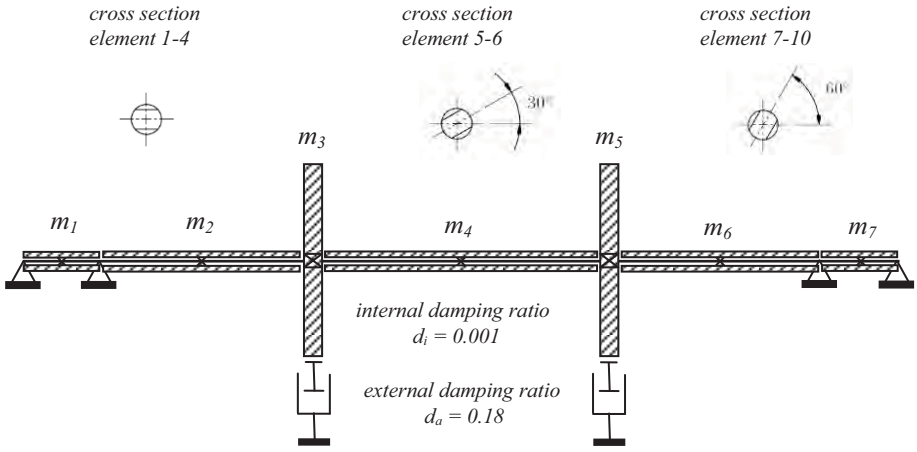

Figure 3: Mathematical model 2 of the rotor

ISSN 1411-1284

Table 2: Parameter of discrete shaft element (model 2).

No. element	Length of element [m]	Modulus of elasticity [MPa]	Orientation of shaft element [degree]	Mass of disk/shaft element [kg]	Polar mass moment of inertia, Θ_p [kgm^2]	Axial mass moment of inertia, Θ_a [kgm^2]
1	0.025	210E+9	0	m_1= 0.015	0.0000001224	0.0000008581
2	0.025	210E+9	0			
3	0.065	210E+9	0	m_2 = 0.039	0.0000003096	0.0000021704
4	0.065	210E+9	0			
-	-	-	-	m_3 = 1.153	0.0025720000	0.0013560000
5	0.090	210E+9	30	m_4 = 0.054	0.0000004320	0.0000030285
6	0.090	210E+9	30			
-	-	-	-	m_5 = 1.153	0.0025720000	0.0013560000
7	0.065	210E+9	60	m_6 = 0.039	0.0000003096	0.0000021704
8	0.065	210E+9	60			
9	0.025	210E+9	60	m_7 = 0.015	0.0000001224	0.0000008581
10	0.025	210E+9	60			

3.RESULTS AND DISCUSSION

In this presented work, the natural frequencies and the dynamic responses of the rotor will be analyzed. In the experimental results, the natural frequencies of the rotor are obtained from the free vibrations of the rotor at rest excited by an impact force at disk 2 in *z*-direction. In the numerical results, the natural frequencies are obtained by solving the eigenvalues of the homogenous linear equation of the rotor in eq.1. Comparing the natural frequencies of the rotor as presented in table 3,the four lower natural frequencies of the rotor in the numerical result in the rotor model 1 are rather higher than the experimental result. Note that, for simplification in comparison of the natural frequencies, the third and the fourth natural frequencies both in the experimental result and the numerical result of the rotor model 1 are listed as the fifth and the sixth natural frequencies in table 3. In the numerical result of the rotor model 2, the six lower natural frequencies of the rotor are slightly lower than the natural frequencies of the rotor model 1, because the mass of shaft elements is taken into account and this mass contributes to reduce the natural frequencies. An alternative way in modeling of anisotropic rotor, whereas there is no change of the number of degrees of freedom of the rotor model and the number of discrete shaft elements: the mass of shaft is added in the mass of disk of the rotor, directly. The result of the first natural frequency of the modified rotor model 1 is only slightly higher than the first natural frequency of the rotor model 2. The second natural frequency of the modified rotor model 1 is only slightly decreased. However, the third and the fourth natural frequencies of the modified rotor model 1 (i.e. listedat the fifth and the sixth natural frequencies in table 3) tend to close to the experimental results.

Table 3: Comparison of natural frequencies

Natural frequency	Experimental [Hz]	Numerical (model 1) [Hz]	Numerical (model 2) [Hz]	Numerical (modified model 1) [Hz]
1	21	25.3	24.3	24.5
2	26	33.5	25.7	32.5
3	-	-	33.5	-
4	-	-	38.6	-
5	55	55.7	55.4	53.9
6	68	72.8	72.5	70.6

Furthermore, the dynamic responses of the rotor especially in the experimental results only the displacement of the disk 2 will be analyzed, because the responses of the disk 2 shows the better signal than the signal at disk 1. This may be caused by two possibilities. First, it may be caused by the coupling (see figure 1) which holds the free motion of the shaft end. Therefore, a bending moment occurs in the bearing which reduces the displacement near this bearing. For the disk 2, this effect is small because of the larger distance to the bearing. Second, it may be caused by a misalignment or bowing at the shaft center line.
In the dynamic responses analyses, the signal in time domain is transformed into frequency domain by using Fast Fourier Transform (FFT) in the MATLAB software. At each rotating speed of the rotor from 1 Hz to 80 Hz with an incremental speed of 1 Hz, the Ω and 2Ω components of the signal are separated. At each frequency ofthe Ω and 2Ω signal components, the maximum amplitudes are recorded and presented as shown in figure 4. In this figure, the dynamic responses of the rotor model 2 cannot be reached, because the difference between the biggest and the smallest of mass components in the mass matrix is too high, therefore the time interval Δt in the numerical simulation should be very small. The problem occurs in a calculation accuration and in a computational time.

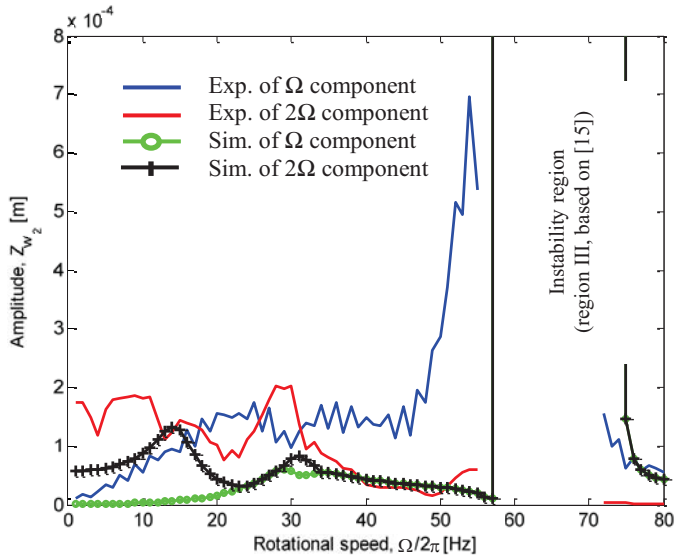

Figure 4: Comparison of the experimental and numerical simulation results (model 1)of the dynamic responses of the disk 2 (Z_{w2})

The responses of the disk 2 in figure 4 tend to similar results which have three separated regions of instability as shown for the rotor cases in [15]. The first region of instability corresponds to the region between the first and the second natural frequency and the third instability region to the third and the fourth natural frequency with a shift to higher frequencies. However, the response amplitudes in the first region (18-27 Hz) as listed in table 4 and the second region (34-38 Hz) do not show unstable responses. It was verified experimentally in figure 4 that the rotor may be influenced by higher damping coefficient especially by the external dampers. The instability region of the experimental results occur only in the third region at frequencies 56-71 Hz, whereas in the numerical results of the rotor model 1 at frequencies 58-74 Hz and in the modified rotor model 1 at frequencies 55-72 Hz. Here, the third instability interval of the experimental result is narrower than the one of the numerical results.

Furthermore, the comparison of the regions with the relatively higher amplitudes or instability regions based on the Ω component of the responses in the disk 2 is listed in table 4. The responses in the experimental results at rotational speeds around 18-27 Hz and around 34-38 Hz occur with the moderately higher amplitudes, whereas the moderately higher amplitudes in the numerical results occur at rotational speed around 27-28 Hz and 33-35 Hz in the rotor model 1 and 24-26 Hz and 33-35 Hz in the modified rotor model 1. Generally, the numerical results of the modified rotor model 1 tend to similar to the result of the rotor model 1.

Table 4: Comparison of the relatively higher amplitudes or the instability regions based on the Ω component of the responses atdisk 2

Region	Experimental [Hz]	Numerical (model 1) [Hz]	Numerical (model 2) [Hz]	Numerical (modified model 1) [Hz]
1	18-27(*)	27-28(*)	n.a.	24-26(*)
2	34-38(*)	33-35(*)	n.a.	33-35(*)
3	56-71	58-74	n.a.	55-72

(*) the response amplitude in this region is moderately high only (not unstabtable)

Finally, the 2Ω component of the experimental results is compared to the numerical results. In the experimental results, the peaks of the 2Ω component occur at frequencies 15 Hz and 30 Hz, whereas in the numerical results at frequencies 14.6 Hz and 30.8 Hz. This comparison is listed in table 5. At lower rotational speeds (i.e. rotational speeds from Ω=0 to 12 Hz), the 2Ω components of the experimental result in figure 4 show the higher amplitudes compared to the numerical result. In the numerical result, the deflections of the rotor at lower rotational speeds are caused by the anisotropy of the shaft, whereas the greater deflections in the experimental results are caused not only by the anisotropy of the shaft but also by the misalignment or bowing in the shaft. Therefore, measured data up to 12 Hz were neglected in the following analysis.

Table 5: Comparison of the peaks of the 2Ω component of the responses at the disk 2

Peak	Experimental [Hz]	Numerical (model 1) [Hz]	Numerical (model 2) [Hz]	Numerical (modified model 1) [Hz]
1	15	14.6	n.a.	13.5
2	30	30.8	n.a.	30.0

ISSN 1411-1284

4. CONCLUSION

Based on the experimental and numerical simulation results, generally, the dynamic responses of the anisotropic rotor are dominated by Ω and 2Ω components of the rotating disk speeds. Because of anisotropy of the rotor the instabilities occur in the wide range with the sharp boundary of the rotating disk speeds. Comparing the numerical and the experimental results, the natural frequencies of the numerical results of the first model is rather higher than the experimental results. The better results which closed to the experimental results are obtained in the second rotor model, where the mass of shaft is taken into account, therefore, they contributes to reduce the natural frequencies. However, the rotor model, in which the mass of element is distributed into mass of discrete shaft element, therefore the number of discrete shaft element and the degrees of freedom of the rotor system increase,thus the computational time will increase significantly. Besides, the numerical problem will occur in the simulation of the dynamic responses if the mass of disk and the mass of shaft is too different each other. A better alternative way in modeling of anisotropic rotor, whereasthere is no change of the number of degrees of freedom of the rotor model and the number of discrete shaft elements: the mass of shaft is added in the mass of disk of the rotor, directly.

ACKNOWLEDGMENT

The author is grateful to the Indonesian National Higher Education which has funded this current researchthrough the Research Unit of the Andalas University with "Fundamental Research Fund 2013"

REFERENCES

[1] Kellenberger, *Biegeschwingungeneinerunrunden, rotierendenWelle in horizontalerLage*, Ingenieur-Archiv26, 1958, pp. 302-318.
[2] E. H. Hull, *Shaft Whirling as Influenced by Stiffness Asymmetry*, ASME Journal of Engineering for Industry 83 (1961), pp. 219-226.
[3] S. T. Ariaratnam, *The Vibration of Unsymmetrical Rotating Shafts*, Journal of Applied Mechanics, Transactions of ASME, Mar. 1965, pp. 157-162.
[4] T. Yamamoto, H. Ota, K. Kono, On *the Unstable Vibrations of a Shaft with Unsymmetrical Stiffness Carrying an Unsymmetrical rotor*, Journal of Applied Mechanics, 35 (1968), pp. 313-321.
[5] J. Michatz, *Das Biegeverhalteneinereinfachbesetzten, unrundenrotierendenWelleunterBerücksichtigungäußerer und innererDämpfungeinflüsse*, Dissertation an der TU Berlin, 1970.
[6] H. L. Wettergren, K.-O. Olsson, *Dynamic Instability of a Rotating Asymmetric Shaft with Internal Viscous Damping Supported in Anisotropic Bearings*, Journal of Sound and Vibration, 195 (1), pp. 75-84, 1996.
[7] N. Bachschmid, P. Pennacchi, Theoretical model results of rub in real rotating maschinery, Proceedings of the XII International Symposium on Dynamic Problems of Mechanics (DINAME 2007), Brazil, February 26-Mar 2, 2007.
[8] J. Malta,,*PemetaanKestabilanTurbin Gas Horizontal denganPendekatan Rotor Multi Disks*, Proceeding of SNTTM XI Yogyakarta, 2012, MT-042.
[9] Chen, L.-W., Peng, W.-K., *Stability Analyses of a Timoshenko Shaft with Dissimilar Lateral Moments of Inertia*, Journal of Sound and Vibration, (1997) 207(1), pp. 33-46.
[10] Oncescu, F., Lakis, A.A., Ostiguy, G., *Investigation of the Stability and Steady State Response of Asymmetric Rotors using Finite Element Formulation*, Journal of Sound and Vibration (2001) 245 (2), pp. 303-328.
[11] F. E. Boru, and H. Irretier, *Numerical and Experimental Dynamic Analysis of a Rotor with Non-Circular Shaft Mounted in Anisotropic Bearings*, SIRM 2009-8th International Conference on Vibrations in Rotating Machines, Vienna, Austria, 23-25 February 2009.
[12] J. Malta, *Effect of different shaft orientation due to stability of anisotropic rotor*, JurnalTeknikMesin Indonesia Vol. 5 No. 2, October 2010, pp. 127-133.
[13] Accelerated Anisotropic Rotor through its Critical Speeds, Proceeding SNTTM 9 Palembang, 13-15 October 2010.
[14] R. Gasch, K. Knothe, *Strukturdynamik, Band 1: DiskreteSysteme*, Berlin Heidelberg: Springer-Verlag, 1987.
[15] J. Malta, *Stability Investigation of Anisotropic Rotor with Different Shaft Orientation Supported by Anisotropic Bearings*, Proceeding of Seminar NasionalTahunanTeknikMesin (SNTTM ke-9) Palembang, 13-15 October 2010, p. MIII:23-30.